organics

MDPI

Article

How Do Positions of Phosphito Units on a Calix[4]Arene Platform Affect the Enantioselectivity of a Catalytic Reaction?

Shaima Hkiri and David Sémeril *

Synthèse Organométallique et Catalyse, UMR-CNRS 7177, Institut de Chimie de Strasbourg, Université de Strasbourg, 4 rue Blaise Pascal, 67008 Strasbourg, France

* Correspondence: dsemeril@unistra.fr; Tel.: +33-(0)3-6885-1519

Abstract: Three chiral diphosphites, (*S*,*S*)-5,17-bis(1,1′-binaphthyl-2,2′-dioxyphosphanyloxy)-25,26,27,28-tetrapropyloxycalix[4]arene (**1**), (*S*,*S*)-5,11,17,23-tetra-*tert*-butyl-25,27-dipropoxy-26,28-bis(1,1′-binaphthyl-2,2′-dioxyphosphanyloxy)calix[4]arene (**2**) and (*S*,*S*)-5,11,17,23-tetra-*tert*-butyl-25,26-dipropoxy-27,28-bis(1,1′-binaphthyl-2,2′-dioxyphosphanyloxy)calix[4]arene (**3**), based on conical calix[4]arene were investigated in the rhodium-catalyzed asymmetric hydrogenation of α-dehydroamino esters. High conversions were observed after 24 h under 5 bar of hydrogen whatever the employed diphosphite, and the chiral induction increases in the order **1** < **3** < **2**. This may be due to the presence of the calix[4]arene moiety, which by its presence modifies the second coordination sphere of the catalytic center. The larger steric hindrance around the rhodium atom leads to the higher enantiomeric excess.

Keywords: calix[4]arene; phosphite; rhodium; asymmetric hydrogenation; homogenous catalysis

1. Introduction

Since the rational synthetic methods developed by Gutsche 45 years ago via precise cyclocondensation reactions of *para*-substituted phenols with formaldehyde [1–4], calix[4]arene has become a preferred semi-rigid platform for the preparation of convergent ligands [5–9]. Among these, phosphorus-based ligands are often used in transition metal chemistry in particular for catalytic applications [10,11]. The phosphorus atom(s) can be specifically grafted on the upper [12–20] or lower [21–30] rim of the calix[4]arene.

Due to the intrinsic properties of calixarene, its incorporation in the ligand structure presents many advantages such as stabilization of the active species thanks to the steric hindrance generated by the macrocycle [31] or by additional interactions with the auxiliary chains [32,33], increased regioselectivity of the reaction by encapsulation of the catalytic center [34,35], inherent chirality of the calixarene leading to optically active ligands [36–38], intrinsic dynamics of the metal center which allow speeding up elementary steps of catalytic cycles [39,40], supramolecular catalysis by trapping the aromatic substrate in its cavity [41], etc. However, the study of the structure–activity relationship is rarely studied; especially from the point of view of academic research, the understanding of the mechanistic aspects needs to be improved. In fact, the position of the phosphorus atom(s) on the calixarenyl platform can drastically affect the coordination sphere of the metal and the catalytic outcome as observed, for example, in the oligomerization of ethylene [42] with tetrahedral [NiX_2(diphosphine)] (X = Cl or Br) complexes, namely *cis*-*P*,*P*′-dibromo{5,17-dibromo-11,23-bis(diphenylphosphino)-25,26,27,28-tetrapropyl-oxycalix[4]arene}nickel [43] (**A**) and *cis*-*P*,*P*′-dichloro-{5,11,17,23-tetra-*tert*-butyl-25,26-bis(diphenylphosphino-methoxy)-27,28-dihydroxycalix[4]arene}nickel [44] (**B**) using methylaluminoxane as an activator (Figure 1). While pre-catalyst **A** led to the formation of butenes, C_4–C_{12} oligomers with a Schulz–Flory distribution (α = 0.22) were obtained when complex **B**, which has a significantly higher steric hindrance, was employed.

check for updates

Citation: Hkiri, S.; Sémeril, D. How Do Positions of Phosphito Units on a Calix[4]Arene Platform Affect the Enantioselectivity of a Catalytic Reaction? *Organics* **2022**, *3*, 470–480. https://doi.org/10.3390/org3040030

Academic Editor: Tomasz K. Olszewski

Received: 13 June 2022
Accepted: 12 October 2022
Published: 9 November 2022

Publisher's Note: MDPI stays neutral with regard to jurisdictional claims in published maps and institutional affiliations.

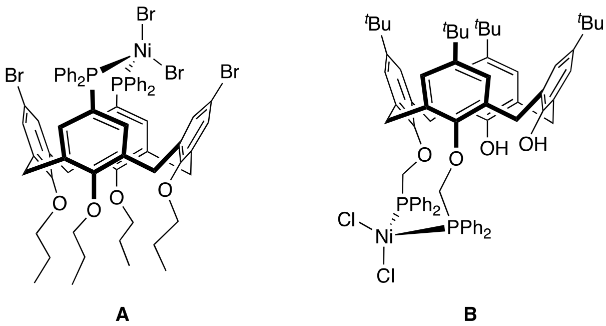

Figure 1. Nickel complexes **A** and **B** for oligomerization of ethylene.

The possibility of fine tuning the coordination sphere of a catalytic center with the calixarenyl preorganization platform allows the modulation of the steric properties of the ligand to a specific reaction. In this context, we now report the use of calixarenyl diphosphites **1–3** for the asymmetric hydrogenation of α-dehydroamino esters (Figure 2). The objective of this work is to relate the positioning of the phophito units on the macrocycle to the efficiency of the chirality transfer from the ligand to the substrates.

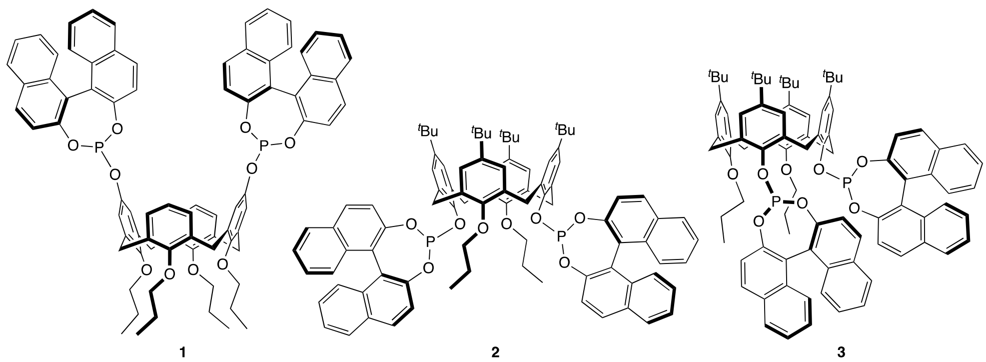

Figure 2. Calixarenyl diphosphites **1–3** employed in the present study.

2. Materials and Methods

All manipulations were carried out under dry argon. Routine ^{1}H, $^{13}C\{^{1}H\}$ and $^{31}P\{^{1}H\}$ spectra were recorded with Bruker FT instruments (AC 300 and 400). ^{1}H NMR and $^{13}C\{^{1}H\}$ spectra were referenced to residual protonated solvents (δ = 7.16 ppm and 128.08 ppm for C_6D_6, respectively, and 7.26 ppm and 77.16 ppm for $CDCl_3$, respectively). ^{31}P NMR spectroscopic data are given relative to external H_3PO_4. Chemical shifts and coupling constants are reported in ppm and Hz, respectively. Mass spectra were recorded on a Bruker MicroTOF spectrometer (ESI-TOF). The catalytic solutions were analyzed by using a Varian 3900 gas chromatograph equipped with a CHROMPAK chiral fused silica Chirasil-L-Val column (25 m × 0.25 mm). (*S*,*S*)-5,17-Bis(1,1′-binaphthyl-2,2′-dioxyphosphanyloxy)-25,26,27,28-tetrapropyloxycalix[4]arene (**1**) [45] and (*S*,*S*)-5,11,17,23-tetra-*tert*-butyl-25,27-dipropoxy-26,28-bis(1,1′-binaphthyl-2,2′-dioxyphosphanyl-oxy)calix[4]arene (**2**) [46] were prepared by literature procedures.

2.1. Synthesis of 5,11,17,23-Tetra-tert-butyl-25,26-dipropyloxy-27,28-dihydroxycalix[4]arene (**4**) *[47]*

First, 15,16,17,18-tetra-*tert*-butyl-25,26,27,28-tetrahydroxycalix[4]arene (2.500 g, 3.8 mmol) dissolved in DMF (500 mL) at 50 °C was deprotonated with NaH (60% dispersion in oil; 0.770 g, 19.3 mmol). After 0.5 h, ^{n}PrBr (1.050 g, 0.78 mL, 8.5 mmol) was added, and the reaction mixture was heated at 60 °C. After 4 days, the solvent was evaporated to dryness, and the solid residue was solubilized in CH_2Cl_2 (100 mL). The resulting suspension was washed with HCl (2 N, 100 mL). The aqueous layer was extracted with CH_2Cl_2 (2 × 50 mL). The combined organic layers were dried over $MgSO_4$ and concentrated. The desired

white solid product was precipitated by addition of methanol, filtered off and dried under vacuum (1.692 g, 60%). ^{1}H NMR (300 MHz, $CDCl_3$): δ = 8.89 (s, 2H, OH), 7.00 (d, 2H, CH arom, ^{4}J = 2.4 Hz), 6.98 (d, 2H, CH arom, ^{4}J = 2.8 Hz), 6.97 (d, 2H, CH arom, ^{4}J = 2.8 Hz), 6.91 (d, 2H, CH arom, ^{4}J = 2.4 Hz), 4.49 and 3.32 (AB system, 2H, $ArCH_2Ar$, ^{2}J = 12.6 Hz), 4.32 and 3.34 (AB system, 4H, $ArCH_2Ar$, ^{2}J = 12.9 Hz), 4.29 and 3.32 (AB system, 2H, $ArCH_2Ar$, ^{2}J = 13.2 Hz), 4.08–4.00 (m, 2H, OCH_2), 3.90–3.82 (m, 2H, OCH_2), 2.08 (hex, 4H, CH_2CH_3, ^{3}J = 7.5 Hz), 1.26 (s, 18H, $C(CH_3)_3$), 1.12 (t, 6H, CH_2CH_3, ^{3}J = 7.5 Hz), 1.10 (s, 18H, $C(CH_3)_3$) ppm.

*2.2. Synthesis of (S,S)-5,11,17,23-Tetra-tert-butyl-25,26-dipropoxy-27,28-bis(1,1′-binaphthyl-2,2′-dioxyphosphanyloxy)calix[4]arene (**3**)*

Here, 5,11,17,23-tetra-*tert*-butyl-25,26-dipropyloxy-27,28-dihydroxycalix[4]arene (**4**) (0.600 g, 0.82 mmol) in refluxing toluene (30 mL) was deprotonated with NaH (60% dispersion in oil, 0.072 g, 1.80 mmol). After 24 h, a solution of [(*S*)-(1,1′-binaphthalene-2,2′-diyl)]chlorophosphite (0.718 g, 2.05 mmol) in toluene (15 mL) was added at 0 °C. The resulting reaction mixture was stirred at room temperature for an additional 2 h. The crude solution was filtered through Al_2O_3, which was washed twice with toluene (2 × 15 mL). The desired white solid product **3** was obtained by evaporation of the toluene under reduced pressure (0.792 g, yield 71%). ^{1}H NMR (300 MHz, C_6D_6): δ = 8.10 (d, 1H, CH arom, ^{3}J = 8.7 Hz), 7.78 (d, 1H, CH arom, ^{3}J = 8.7 Hz), 7.71 (d, 1H, CH arom, ^{3}J = 8.1 Hz), 7.63 (d, 1H, CH arom, ^{3}J = 8.1 Hz), 7.60–7.53 (m, 3H, CH arom), 7.47 (d, 1H, CH arom, ^{3}J = 8.7 Hz), 7.29–7.22 (m, 4H, CH arom), 7.13–7.02 (m, 12H, CH arom), 7.00–6.93 (m, 3H, CH arom), 6.92–6.90 (m, 2H, CH arom), 6.76 (brs, 2H, CH arom), 6.03 (brs, 1H, CH arom), 5.32 and 3.48 (AB system, 2H, $ArCH_2Ar$, ^{2}J = 13.2 Hz), 4.97 and 3.46 (AB system, 2H, $ArCH_2Ar$, ^{2}J = 12.9 Hz), 4.34 and 3.14 (AB system, 2H, $ArCH_2Ar$, ^{2}J = 12.3 Hz), 4.32 and 3.38 (AB system, 2H, $ArCH_2Ar$, ^{2}J = 13.5 Hz), 3.78–3.52 (m, 4H, OCH_2), 1.81–1.66 (m, 4H, CH_2CH_3), 1.45 (s, 9H, $C(CH_3)_3$), 1.39 (s, 9H, $C(CH_3)_3$), 1.09 (s, 9H, $C(CH_3)_3$), 0.99 (s, 9H, $C(CH_3)_3$), 0.95 (t, 3H, CH_2CH_3, ^{3}J = 7.4 Hz), −0.17 (t, 3H, CH_2CH_3, ^{3}J = 7.5 Hz); ^{13}C{^{1}H} NMR (75 MHz, C_6D_6): δ = 154.30–122.35 (arom C's), 78.38 (s, OCH_2), 76.28 (s, OCH_2), 34.31 (s, $C(CH_3)_3$), 34.15 (s, $C(CH_3)_3$), 34.01 (s, $C(CH_3)_3$), 32.81 (s, $ArCH_2Ar$), 32.61 (s, $ArCH_2Ar$), 32.36 (s, $ArCH_2Ar$), 32.11 (s, $C(CH_3)_3$), 31.96 (s, $C(CH_3)_3$), 31.55 (s, $ArCH_2Ar$), 31.40 (s, $C(CH_3)_3$), 23.62 (s, CH_2CH_3), 22.90 (s, CH_2CH_3), 10.92 (s, CH_2CH_3), 8.84 (s, CH_2CH_3); ^{31}P{^{1}H} NMR (121 MHz, C_6D_6): δ = 150.7 (s, $OP(OAr)_2$) ppm. Elemental analysis (%): calcd for $C_{90}H_{90}P_2O_8$ (1361.62): C 79.39, H 6.66; found: C 79.16, H 6.84.

*2.3. Synthesis of cis-P,P′-{[(S,S)-5,11,17,23-Tetra-tert-butyl-25,27-dipropyloxy-26,28-bis(1,1′-binaphtyl-phosphite)calix[4]arene]-1,5-cyclooctadiene}rhodium(I) Tetrafluoroborate (**5**)*

Ligand **2** (0.284 g, 0.21 mmol) in CH_2Cl_2 (5 mL) was added drop to drop to a solution of $[Rh(cod)_2]BF_4$ (0.077 g, 0.19 mmol) in CH_2Cl_2 (250 mL). After 16 h, the resulted solution was concentrated to ca. 3 mL, and the complex **5** was precipitated out after the addition of hexane (50 mL). The orange precipitate was filtered off and dried under vacuum (0.280 g, 89% yield). ^{1}H NMR (300 MHz, $CDCl_3$): δ = 8.24 (d, 2H, CH arom, ^{3}J = 8.8 Hz), 8.03 (d, 2H, CH arom, ^{3}J = 8.8 Hz), 7.99 (d, 2H, CH arom, ^{3}J = 8.1 Hz), 7.78 (d, 2H, CH arom, ^{3}J = 8.1 Hz), 7.68 (d, 2H, CH arom, ^{3}J = 8.9 Hz), 7.51–7.35 (m, 6H, CH arom), 7.24–7.10 (m, 4H, CH arom), 6.98 (d, 2H, CH arom, ^{3}J = 8.6 Hz), 6.86 (d, 2H, CH arom, ^{3}J = 8.6 Hz), 6.79 (d, 2H, CH arom, ^{4}J = 2.1 Hz), 6.58 (d, 2H, CH arom, ^{4}J = 2.4 Hz), 6.28 (d, 2H, CH arom, ^{4}J = 2.1 Hz), 6.23 (d, 2H, CH arom, ^{4}J = 2.1 Hz), 6.19–6.09 (m, 2H, CH of cod), 5.01 and 2.98 (AB system, 4H, $ArCH_2Ar$, ^{2}J = 13.5 Hz), 4.89 and 3.31 (AB system, 4H, $ArCH_2Ar$, ^{2}J = 12.7 Hz), 4.46-4.38 (m, 2H, OCH_2), 4.36–4.23 (m, 2H, CH of cod), 4.11–3.97 (m, 2H, OCH_2), 2.74–2.58 (m, 2H, CH_2 of cod), 2.40–2.33 (m, 2H, CH_2 of cod), 2.33–2.10 (m, 4H, CH_2CH_3), 1.65–1.53 (m, 2H, CH_2 of cod), 1.16 (t, 6H, CH_2CH_3, ^{3}J = 7.4 Hz), 1.09–1.04 (m, 2H, CH_2 of cod), 1.01 (s, 18H, $C(CH_3)_3$), 0.74 (s, 18H, $C(CH_3)_3$); ^{13}C{^{1}H} NMR (75 MHz, $CDCl_3$): δ = 151.16–119.71 (arom Cs), 106.66 (s, CH of cod), 95.99 (s, CH of cod), 77.92 (s, OCH_2), 34.97 (s, CH_2 of cod), 33.69 (s, $C(CH_3)_3$), 33.61 (s, CH_2 of cod), 33.60 (s, $ArCH_2Ar$), 33.61 (s, CH_2 of

cod), 33.58 (s, $C(CH_3)_3$), 33.36 (s, $ArCH_2Ar$), 31.10 (s, $C(CH_3)_3$), 30.90 (s, $C(CH_3)_3$), 26.79 (s, CH_2 of cod), 23.54 (s, CH_2CH_3), 10.27 (s, CH_2CH_3); $^{31}P\{^1H\}$ NMR (121 MHz, $CDCl_3$): δ = 120.7 (d, $OP(OAr)_2$, $^1J_{P\text{-}Rh}$ = 256.8 Hz) ppm. MS (ESI TOF), m/z: 1571.61 $[M–BF_4]^+$ and 1463.54 $[M–C_8H_{12}–BF_4]^+$ expected isotopic profiles. Elemental analysis (%): calcd for $C_{98}H_{102}BF_4O_8P_2Rh$ (1659.51): C 70.93, H 6.19; found: C 70.86, H 5.94.

2.4. General Procedure for the Hydrogenation Experiments

Hydrogenation experiments were carried out in a glass-lined, 100 mL stainless steel autoclave containing a magnetic stirring bar. The reactor was flushed with nitrogen and charged with $[Rh(cod)_2]BF_4$ (0.01 mmol), ligand (0.01 mmol) and CH_2Cl_2 (10 mL). The resulting mixture was stirred at room temperature for 0.5 h. The α-dehydroamino esters (1.00 mmol) were then added. The autoclave was flushed twice with H_2, pressurized to 5 bars and stirred at room temperature for 24 h. After depressurization of the reactor, the solution was passed through a short silica column to remove the catalyst. The conversion and the enantioselectivity were determined by ^1H NMR spectroscopy and by chiral GC analysis using a CHROMPAK chiral fused silica Chirasil-L-Val column (25 m × 0.25 mm), respectively.

N-Acetyl-phenylalanine methyl ester (**7a**) ^1H NMR ($CDCl_3$, 300 MHz): δ = 7.31–7.21 (m, 3H, CH arom), 7.09 (dd, 2H, CH arom, ^3J = 7.7 Hz, ^4J = 1.9 Hz), 6.05 (d, 1H, NH, ^3J = 7.8 Hz), 4.87 (dt, 1H, CH_2CHNH, ^3J = 7.8 Hz, ^3J = 5.8 Hz), 3.71 (s, 3H, CO_2CH_3), 3.12 and 3.09 (ABX system, 2H, CH_2CH, ^2J = 13.8 Hz, ^3J = 5.8 Hz), 1.97 (s, 3H, $NHCOCH_3$) ppm.

N-Acetyl-4-fluoro-phenylalanine methyl ester (**7b**) ^1H NMR ($CDCl_3$, 300 MHz): δ = 7.07–6.93 (m, 4H, CH arom), 6.02 (d, 1H, NH, ^3J = 7.6 Hz), 4.85 (dt, 1H, CH2CHNH, ^3J = 7.6 Hz, ^3J = 5.7 Hz), 3.71 (s, 3H, CO_2CH_3), 3.12 and 3.04 (ABX system, 2H, CH_2CH, ^2J = 14.1 Hz, ^3J = 5.7 Hz), 1.98 (s, 3H, $NHCOCH_3$) ppm.

N-Acetyl-4-chloro-phenylalanine methyl ester (**7c**) ^1H NMR ($CDCl_3$, 300 MHz): δ = 7.23 (d, 2H, CH arom, ^3J = 8.3 Hz), 7.01 (d, 2H, CH arom, ^3J = 8.3 Hz), 6.18 (brs, 1H, NH), 4.83 (dt, 1H, CH_2CHNH, ^3J = 7.8 Hz, ^3J = 5.8 Hz), 3.69 (s, 3H, CO_2CH_3), 3.98 and 3.01 (ABX system, 2H, CH_2CH, ^2J = 13.8 Hz, ^3J = 5.8 Hz), 1.95 (s, 3H, $NHCOCH_3$) ppm.

N-Acetyl-3,4-dichloro-phenylalanine methyl ester (**7d**) ^1H NMR ($CDCl_3$, 300 MHz): δ = 7.33 (d, 1H, CH arom, ^3J = 8.3 Hz), 7.18 (d, 1H, CH arom, ^4J = 2.2 Hz), 6.93 (dd, 1H, CH arom, ^3J = 8.3 Hz, ^4J = 2.2 Hz), 6.19 (d, 1H, NH, ^3J = 7.6 Hz), 4.85 (dt, 1H, CH_2CHNH, ^3J = 7.6 Hz, ^3J = 5.9 Hz), 3.72 (s, 3H, CO_2CH_3), 3.11 and 2.99 (ABX system, 2H, CH_2CH, ^2J = 13.9 Hz, ^3J = 5.9 Hz), 1.98 (s, 3H, $NHCOCH_3$) ppm.

3. Results

Starting from the 5,11,17,23-tetra-*tert*-butyl-25,26,27,28-tetrol-calix[4]arene, two diphosphites in which the phosphito units are grafted on distal aromatic either on the upper or on the lower rim of the macrocycle, namely (*S*,*S*)-5,17-bis (1,1′-binaphthyl-2,2′-dioxyphosphanyloxy)-25,26,27,28-tetrapropyloxycalix[4]arene (**1**) [45] and (*S*,*S*)-5,11,17,23-tetra-*tert*-butyl-25,27-dipropoxy-26,28-bis(1,1′-binaphthyl-2,2′-dioxyphosphanyloxy)calix[4]arene (**2**) [46] were prepared following previous reports of our group. The third diphosphite was obtained in two steps: firstly, a double alkylation of two proximally phenolic units with NaH and ^{n}PrBr in DMF, which led after 4 days at room temperature to the O-dialkylated precursor **4** [47] in 60% yield. In keeping with a *Cs*-symmetrical structure, its ^1H NMR spectrum displays three distinct AB patterns for the diastereotopic $ArCH_2Ar$ protons at 4.49/3.32 (^2J = 12.6 Hz), 4.32/3.34 (^2J = 12.9 Hz), and 4.29/3.32 (^2J = 13.2 Hz) ppm integrated for 2, 4 and 2 protons, respectively.

The second step consists of a double deprotonation of intermediate with NaH **4** followed by a reaction with (*S*)-(1,1′-binaphthalene-2,2′-diyl)chlorophosphite, which led to the diphosphite **3** (Scheme 1). After workup, diphosphite **3** was isolated in 71% yield and was characterized by a singlet peak at 150.7 ppm in its ^{31}P NMR spectrum. As anticipated, the "cone" conformation of the calix[4]arene was inferred from the corresponding ^{13}C NMR spectrum, which shows four signals in the range 32.81–31.55 ppm for the $ArCH_2Ar$ groups [48].

Consistent with a C_1-symmetrical compound, the ^{1}H NMR spectrum displays four distinct AB patterns for the $ArCH_2Ar$ protons at 5.32/3.48 (^2J = 13.2 Hz), 4.97/3.46 (^2J = 12.9 Hz), 4.34/3.14 (^2J = 12.3 Hz) and 4.32/3.38 (^2J = 13.5 Hz) ppm (see Supplementary Materials).

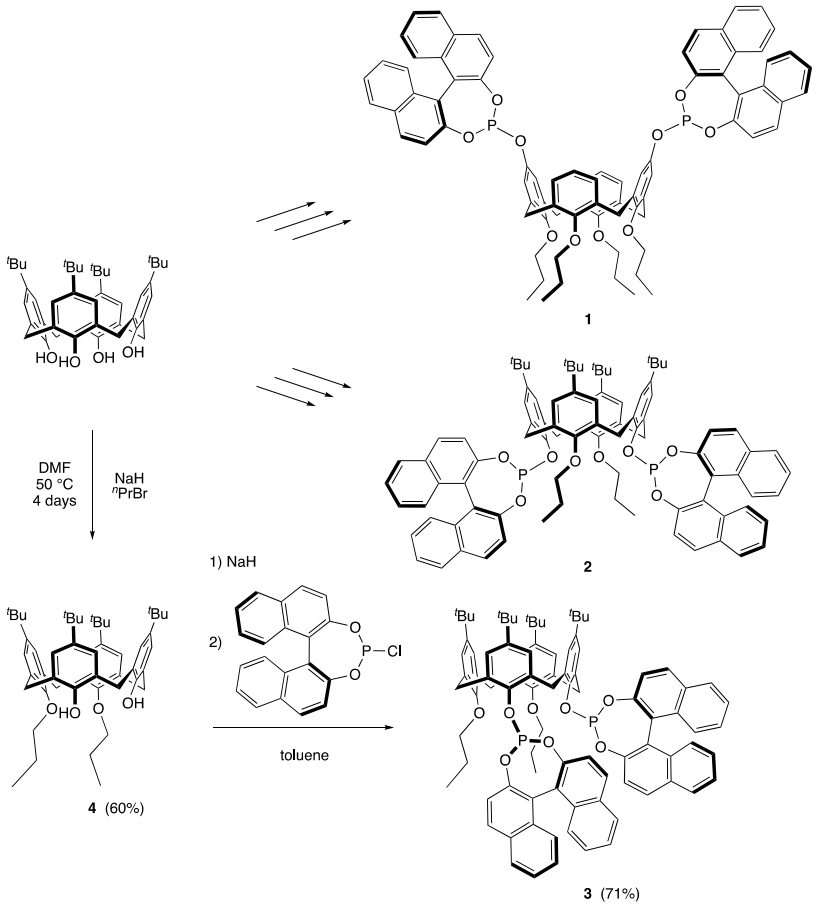

Scheme 1. Synthesis of diphosphites **1**–**3**.

The reaction of the lower rim distally substituted diphosphito-calixarene **2** with $[Rh(cod)_2]BF_4$ (cod = 1,5-cyclooctadiene) in CH_2Cl_2 (0.7 mM) gave, after work-up, the complex **5** in 89% yield as an orange solid (Scheme 2). Owing to the large separation between the two coordinated atoms, 12 bonds, the exclusive formation of a *P*,*P*-chelate rhodium complex occurred. The structure of the complex was deduced from its mass spectrum, which shows strong peaks corresponding to the $[M–BF_4]^+$ and $[M–C_8H_{12}–BF_4]^+$ cations at m/z = 1571.61 and 1463.54, respectively. NMR spectra are consistent with a C_2-symmetrical molecule: a doublet centered at 120.7 ppm ($^1J_{P\text{-}Rh}$ = 256.8 Hz) and two AB systems for the diastereotopic $ArCH_2Ar$ protons at 5.01/2.98 (^2J = 13.5 Hz) and 4.89/3.31 (^2J = 12.7 Hz) ppm are observed in the corresponding ^{31}P and ^{1}H NMR spectra, respectively (see Supplementary Materials). Note that when the synthesis of complex **5** was performed in lower-dilution conditions (10 mM), the formation of by-products was observed (85% purity). Nevertheless, with this mixture of complexes, Sandoval et al. observed important enantiomeric excesses in the asymmetric hydrogenation of methyl-(*Z*)-2-(acetamido)acrylate and methyl-(*Z*)-2-(acetamido)cinnamate [49].

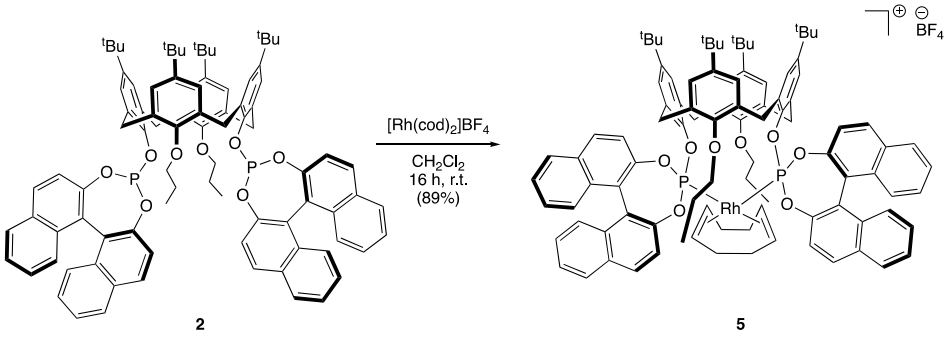

Scheme 2. Formation of [Rh(**2**)(cod)]BF_4 complex (**5**).

Four different α-dehydroamino esters, namely (*Z*)-*N*-acetyl-dehydro-phenylalanine methyl ester (**6a**), (*Z*)-*N*-acetyl-dehydro-4-fluoro-phenylalanine methyl ester (**6b**), (*Z*)-*N*-acetyl-dehydro-4-chloro-phenylalanine methyl ester (**6c**) and (*Z*)-*N*-acetyl-dehydro-3,4-dichloro-phenylalanine methyl ester (**6d**) were used to assess the performance of diphosphites **1**–**3** in the rhodium catalyzed asymmetric hydrogenation (Scheme 3).

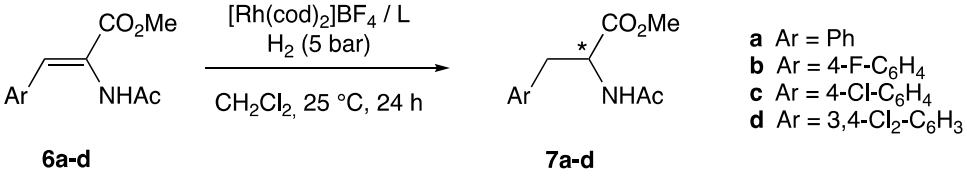

Scheme 3. Enantiomeric hydrogenation of α-dehydroamino esters **6a**–**d**.

In the following tests, the catalytic system was in situ generated by mixing an equimolar amount (0.01 mmol, 1 mol %) of [Rh(cod)$_2$]BF_4 as metal precursor and ligand (**1**–**3**) in CH_2Cl_2. The resulting solution was stirred at room temperature for 30 min before the addition of the α-dehydroamino ester (**6a**–**d**; 1 mmol). The reaction mixture was stirred under 5 bar of hydrogen for an additional 24 h. ^{1}H NMR carried out on the reaction mixtures revealed that using ligands **1**–**3**, the conversion was increased in the order **1** < **2** < **3** (Table 1). As example, under the latter catalytic conditions, (*Z*)-*N*-acetyl-dehydro-4-fluoro-phenylalanine methyl ester (**6b**) was reduced into *N*-acetyl-4-fluoro-phenylalanine methyl ester (**7b**) in 83, 92 and 100% conversion when diphosphites **1**, **2** and **3** were employed, respectively (Table 1, entries 2, 6 and 11).

The reduced products **7a**–**d** were obtained with modest enantiomeric excesses (*ee*) 48–57% when diphosphite **1** was employed (Table 1, entries 1–4). Slightly higher *ee* values, 58–66%, were measured when ligand **3** was used (Table 1, entries 10–13). The more important *ee* values, higher than 90%, were measured when the calixarenyl diphosphite **2** was associated with the rhodium precursor (Table 1, entries 5–8). Using the latter catalytic system, *N*-acetyl-4-chloro-phenylalanine methyl ester (**7c**) and *N*-acetyl-4-fluoro- phenylalanine methyl ester (**7b**) were obtained with *ee* values of 94 and 95%, respectively. Note that under the previous catalytic conditions, repeating the hydrogenation of α-dehydroamino ester **6a** with the well-defined [Rh(**2**)(cod)]BF_4 (**5**) did not change the catalytic outlook; the reduced product **7a** was quantitatively formed (*ee* = 92%) (Table 1, entry 9). No reduction occurred when the dimeric [RhCl(cod)]$_2$ complex was employed as a rhodium source.

Table 1. Enantiomeric hydrogenation of α-dehydroamino esters **6a–d** [1].

Entry		Substrate (Ar)	Ligand	Conversion (%) [2]	*ee* (%) [3]
1	**6a**	(Ar = Ph)	**1**	100	57 (*R*)
2	**6b**	(Ar = 4-F-C_6H_4)	**1**	83	48 (*R*)
3	**6c**	(Ar = 4-Cl-C_6H_4)	**1**	86	57 (*R*)
4	**6d**	(Ar = 3,4-Cl_2-C_6H_3)	**1**	91	52 (*R*)
5	**6a**	(Ar = Ph)	**2**	100	91 (*R*)
6	**6b**	(Ar = 4-F-C_6H_4)	**2**	92	95 (*R*)
7	**6c**	(Ar = 4-Cl-C_6H_4)	**2**	97	94 (*R*)
8	**6d**	(Ar = 3,4-Cl_2-C_6H_3)	**2**	100	90 (*R*)
9 [4]	**6a**	(Ar = Ph)	**2**	100	92 (*R*)
10	**6a**	(Ar = Ph)	**3**	100	62 (*R*)
11	**6b**	(Ar = 4-F-C_6H_4)	**3**	100	66 (*R*)
12	**6c**	(Ar = 4-Cl-C_6H_4)	**3**	100	58 (*R*)
13	**6d**	(Ar = 3,4-Cl_2-C_6H_3)	**3**	100	63 (*R*)

[1] Reagents and conditions: $[Rh(cod)_2]BF_4$ (1 mol %), ligand (1 mol %), CH_2Cl_2 (12 mL), $P(H_2)$ = 5 bar, 25 °C, 24 h; [2] conversions were determined by ^1H NMR spectroscopy (see Supplementary Materials); [3] enantiomeric excess were determinated by chiral GC analysis (CHROMPAK, 25 m × 0.25 mm, Chirasil-L-Val); [4] with [Rh(**2**)(cod)]BF_4 (1 mol %).

It is interesting to note that only a few examples of asymmetric hydrogenation of α-dehydroamino esters using diphosphites derived from optically pure binol were reported. The nature of the bridge linking the two phosphorus atoms has a direct effect on the catalytic outcome. In fact, when D-glucose [50] or *N*-phenyldiethanolamine [51] were incorporated in the ligand, low *ee* values, 28–32%, were measured in the hydrogenation of (*Z*)-*N*-acetyl-dehydro-phenylalanine methyl ester (**6a**). In contrast, important enantiomeric excesses, similar to those obtained with our calixarenyl ligand **2**, were obtained by Fan et al. using diphosphite-containing metallacrown ether as a ligand [52] and by Xia et al. with a norbornane backbone [53].

4. Discussion

As interfered from Table 1, the nature of the diphosphite has a direct influence on the results of the asymmetric hydrogenation of the α-dehydroamino esters **6a–d**; the chiral induction increases in the order **1** < **3** < **2**. Based on the mechanism described by Halpern et al. (Scheme 4) [54–56], these differences would not come from electronic factors (in each case $P(OAr)_3$ moieties) but from steric factors generated by the bridge between the two phosphorus atoms, i.e., by the calix[4]arene platform.

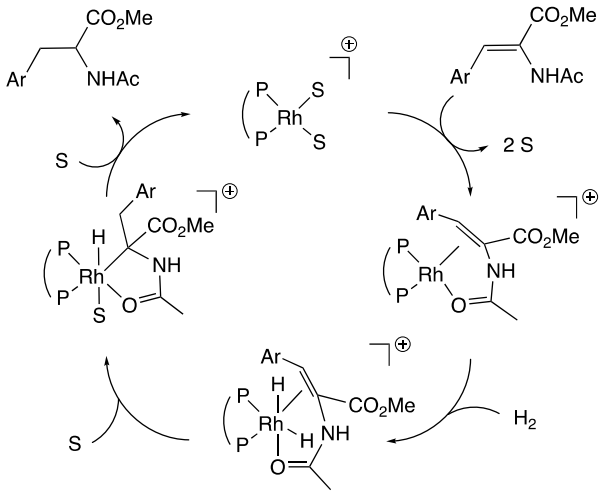

Scheme 4. Halpern's mechanism of hydrogenation.

With the aim of rationalizing the positioning of the phosphito units on the calix[4]arene platform, molecular mechanism calculations using Spartan of [Rh(L)] moieties (L = **1**–**3**), in which the rhodium atom adopts a square-planar coordination geometry, were performed (Figure 3).

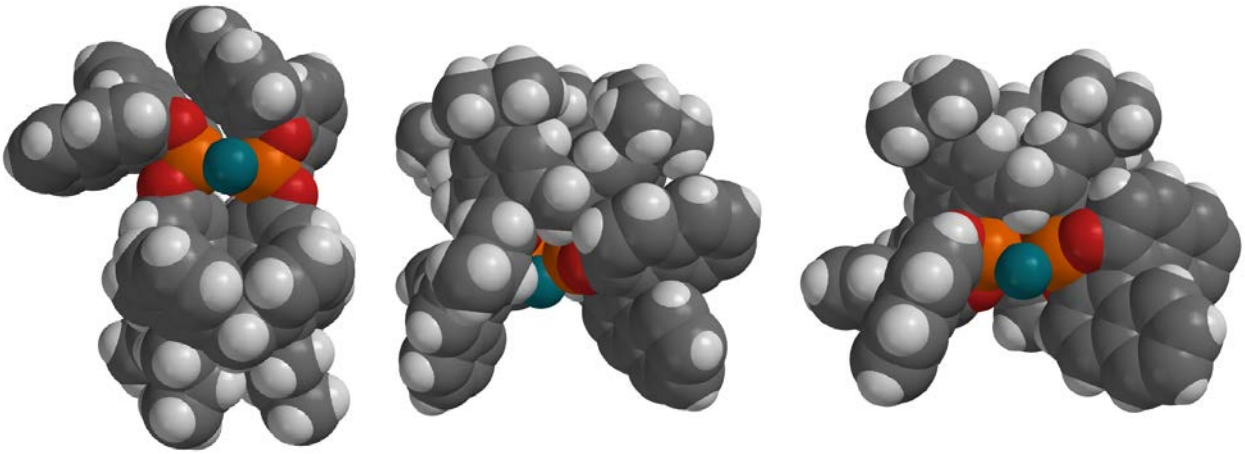

Figure 3. Spartan simulation of [Rh(L)] moieties (L = **1**–**3**) with a rhodium atom (in green) adopting a square-planar coordination geometry.

Simulation of the rhodium complex involving the ligand whose phosphito units are grafted onto the distal aromatics on the upper rim of the calixarene [Rh(**1**)] shows that the rhodium atom is located near the entrance of the macrocyclic cavity. This leads to a largely ligand-free coordination sphere, which is an unfavorable situation for an efficient transfer of chirality from the substituents of the phosphorus atoms to the substrate. In the case of the *P*,*P*-chelate [Rh(**2**)] complex, the rhodium atom was confined in a tight chiral molecular pocket made by the two bulky 1,1′-binaphthalene-2,2′-dioxy moieties and the two auxiliary propyl chains of the calixarene. This feature increases the steric pressure on the catalytic center generated by the optically active phosphite units, which leads to a specific approach of the substrate to the metal allowing an excellent chirality transfer to the *α*-dehydroamino esters. In the case of diphosphite **3** having its phosphorus atoms grafted on two proximally phenolic rings of the calixarene, the rhodium atom mainly adopts an *exo*-orientation with respect to the macrocycle [57]. The simulations indicate that the rhodium atom lies in a sterically hindered environment created by the two phosphito units and by one methylenic moiety of the calixarene. This constrained, asymmetric environment may be responsible for a better efficient chirality transfer than ligand **1**, but it is less efficient when compared to diphosphite **2**.

Regarding the kinetics of the hydrogenation reaction, when substrate (*Z*)-*N*-acetyl-dehydro-4-fluoro-phenylalanine methyl ester (**6b**) or (*Z*)-*N*-acetyl-dehydro-4-chloro-phenyl-alanine methyl ester (**6c**) were employed, the reduction rate increased in the order **1** < **2** < **3**. The most efficient diphosphites are those whose Rh(III)-H intermediates adopt distorted structures due to steric constraints generated by the calix[4]arene (OPr auxiliary groups in **2** and $ArCH_2Ar$ moiety in **3**). This brings the hydride closer to the coordinated olefin or alkyl chain, which promotes both its migration on the olefin and the final reductive elimination step, respectively (Scheme 4).

5. Conclusions

In summary, we have described the synthesis of optically pure diphosphite in which the two phosphorus atoms are grafted on two proximally phenolic rings of a calix[4]arene. The latter compound and two related calixarenyl diphosphites have been employed in the asymmetric hydrogenation of *α*-dehydroamino esters. With these three ligands, high

conversions were observed after 24 h under 5 bar of hydrogen. We have shown that the position of the two phosphito units on the calixarene platform has a determining role in the chirality transfer from the ligand to the substrate and can be directly related to the steric hindrance generated by the second coordination sphere [58] of the ligand, in other words by the calixarenyl skeleton. In fact, the highest enantiomeric excess, 95%, was obtained with diphosphite **2**, which was able to encapsulate the catalytic center inside a molecular pocket generated by the naphthyl substituents and the auxiliary side groups. Further studies aim at exploiting the structural diversity offered by the calix[4]arene platform in homogeneous catalysis.

Supplementary Materials: The following supporting information can be downloaded at: https://www.mdpi.com/article/10.3390/org3040030/s1, ^{1}H, ^{13}C and ^{31}P NMR spectra of compounds **3**–**5** and **7a**–**d** are given.

Author Contributions: Conceptualization, D.S.; investigation, S.H.; formal analysis, S.H.; writing—original draft, S.H.; writing—review and editing, D.S. All authors have read and agreed to the published version of the manuscript.

Funding: This research received no external funding.

Data Availability Statement: Not applicable.

Acknowledgments: We gratefully acknowledge the University of Carthage and the Tunisian Ministry of Higher Education and Scientific Research for the financial support (grant for S.H.).

Conflicts of Interest: The authors declare no conflict of interest.

References

1. Gutsche, C.D.; Muthukrishnan, R. Calixarenes. 1. Analysis of the product mixtures produced by the base-catalyzed condensation of formaldehyde with *para*-substituted phenols. *J. Org. Chem.* **1978**, *43*, 4905–4906. [CrossRef]
2. Gutsche, C.D.; Dhawan, B.; No, K.H.; Muthukrishnan, R. Calixarenes. 4. The synthesis, characterization, and properties of the calixarenes from *p-tert*-butylphenol. *J. Am. Chem. Soc.* **1981**, *103*, 3782–3792. [CrossRef]
3. Gutsche, C.D. Calixarenes. *Acc. Chem. Res.* **1983**, *16*, 161–170. [CrossRef]
4. Gutsche, C.D.; Iqbal, M.; Stewart, D. Calixarenes. 18. Synthesis procedures for *p-tert*-butylcalix[4]arene. *J. Org. Chem.* **1986**, *51*, 742–745. [CrossRef]
5. Wieser, C.; Dieleman, C.B.; Matt, D. Calixarene and resorcinarene ligands in transition metal chemistry. *Coord. Chem. Rev.* **1997**, *165*, 93–161. [CrossRef]
6. Sliwa, W. Calixarene complexes with transition metal, lanthanide and actinide ions. *Croat. Chem. Acta* **2002**, *75*, 131–153.
7. Sliwa, W. Calixarene complexes with transition metal ions. *J. Incl. Phenom. Macrocycl. Chem.* **2005**, *52*, 13–37. [CrossRef]
8. Homden, D.M.; Redshaw, C. The use of calixarenes in metal-based catalysis. *Chem. Rev.* **2008**, *108*, 5086–5130. [CrossRef]
9. Santoro, O.; Redshaw, C. Metallocalix[n]arenes in catalysis: A 13-year update. *Coord. Chem. Rev.* **2021**, *448*, 214173. [CrossRef]
10. Sémeril, D.; Matt, D. Synthesis and catalytic relevance of P(III) and P(V)-functionalised calixarenes and resorcinarenes. *Coord. Chem. Rev.* **2014**, *279*, 58–95. [CrossRef]
11. Bauder, C.; Sémeril, D. Styrene hydroformylation with cavity-shaped ligands. *Eur. J. Inorg. Chem.* **2019**, *47*, 4951–4965. [CrossRef]
12. Hamada, F.; Fukugaki, T.; Murai, K.; Orr, G.W.; Atwood, J.L. Liquid-liquid extraction of transition and alkali metal cations by a new calixarene: Diphenylphosphino calix[4]arene methyl ether. *J. Incl. Phenom. Macrocycl. Chem.* **1991**, *10*, 57–61. [CrossRef]
13. Shimizu, S.; Shirakawa, S.; Sasaki, Y.; Hirai, C. Novel Water-soluble calix[4]arene ligands with phosphane-containing groups for dual functional metal-complex catalysts: The biphasic hydroformylation of water-insoluble olefins. *Angew. Chem. Int. Ed.* **2000**, *39*, 1256–1259. [CrossRef]
14. Fang, X.; Scott, B.L.; Watkin, J.G.; Carter, C.A.G.; Kubas, G.J. Metal complexes based on an upper-rim calix[4]arene phosphine ligand. *Inorg. Chim. Acta* **2001**, *317*, 276–281. [CrossRef]
15. Mongrain, P.; Harvey, P.D. An original calix[4]arene-containing oligomer/polymer catalyst for homogeneous hydroformylation. *Macromol. Rapid Commun.* **2008**, *29*, 1752–1757. [CrossRef]
16. Khiri, N.; Bertrand, E.; Ondel-Eymin, M.-J.; Rousselin, Y.; Bayardon, J.; Harvey, P.D.; Jugé, S. Enantioselective hydrogenation catalysis aided by a σ-bonded calix[4]arene to a *P*-chirogenic aminophosphane phosphinite rhodium complex. *Organometallics* **2010**, *29*, 3622–3631. [CrossRef]
17. Monnereau, L.; Sémeril, D.; Matt, D. High efficiency of cavity-based triaryl-phosphines in nickel-catalysed Kumada-Tamao-Corriu cross-coupling. *Chem. Commun.* **2011**, *47*, 6626–6628. [CrossRef]

18. Khiri-Meribout, N.; Bertrand, E.; Bayardon, J.; Eymin, M.-J.; Rousselin, Y.; Cattey, H.; Fortin, D.; Harvey, P.D.; Jugé, S. P-Chirogenic phosphines supported by calix[4]arene: New insight into palladium-catalyzed asymmetric allylic substitution. *Organometallics* **2013**, *32*, 2827–2839. [CrossRef]
19. Elaieb, F.; Hedhli, A.; Sémeril, D.; Matt, D. Arylcalixarenyl phosphines in palladium-catalyzed Suzuki-Miyaura cross-coupling reactions. *Eur. J. Org. Chem.* **2016**, *10*, 1867–1873. [CrossRef]
20. Elaieb, F.; Sémeril, D.; Matt, D.; Pfeffer, M.; Bouit, P.-A.; Hissler, M.; Gourlaouen, C.; Harrowfield, J. Calix[4]arene-fused phospholes. *Dalton Trans.* **2017**, *46*, 9833–9845. [CrossRef]
21. Csók, Z.; Szalontai, G.; Czira, G.; Kollár, L. Carbonylation (hydroformylation and hydrocarbalkoxylation) reactions in the presence of transition metal: *p-tert*-Butyl-calix[4]arene-based phosphine and phosphinite systems. *J. Organomet. Chem.* **1998**, *570*, 23–29. [CrossRef]
22. Paciello, R.; Siggel, L.; Röper, M. Chelated bisphosphites with a calix[4]arene backbone: New ligands for rhodium-catalyzed low-pressure hydroformylation with controlled regioselectivity. *Angew. Chem. Int. Ed.* **1999**, *38*, 1920–1923. [CrossRef]
23. Jeunesse, C.; Dieleman, C.; Steyer, S.; Matt, D. Calix[4]arene-derived diphosphines, diphosphinites and diphosphites as chelating ligands for transition metal ions. Encapsulation of silver(I) in a calix-crown diphosphite. *J. Chem. Soc. Dalton Trans.* **2001**, *6*, 881–892. [CrossRef]
24. Kunze, C.; Selent, D.; Neda, I.; Freytag, M.; Jones, P.G.; Schmutzler, R.; Baumann, W.; Börner, A. Calix[4]arene-based bis-phosphonites, bis-phosphites, and bis-O-acyl-phosphites as ligands in the rhodium(I)-catalyzed hydroformylation of 1-octene. *Z. Anorg. Allg. Chem.* **2002**, *628*, 779–787. [CrossRef]
25. Marson, A.; Freixa, Z.; Kamer, P.C.J.; van Leeuwen, P.W.N.M. Chiral calix[4]arene-based diphosphites as ligands in the asymmetric hydrogenation of prochiral olefins. *Eur. J. Inorg. Chem.* **2007**, *29*, 4587–4591. [CrossRef]
26. Sémeril, D.; Matt, D.; Toupet, L. Highly regioselective hydroformylation with hemispherical chelators. *Chem. Eur. J.* **2008**, *14*, 7144–7155. [CrossRef]
27. Maji, P.; Mahalakshmi, L.; Krishnamurthy, S.S.; Nethaji, M. Cyclometalated complexes derived from calix[4]arene bisphosphites and their catalytic applications in cross-coupling reactions. *J. Organomet. Chem.* **2011**, *696*, 3169–3179. [CrossRef]
28. Cobley, C.J.; Pringle, P.G. A water-soluble phosphite derived from sulfonated calix[4]arene. The remarkable stability of its rhodium complexes and two phase hydroformylation studies. *Catal. Sci. Technol.* **2011**, *1*, 239–242. [CrossRef]
29. Hirasawa, K.; Tanaka, S.; Horiuchi, T.; Kobayashi, T.; Sato, T.; Morohashi, N.; Hattori, T. Pd(II) Complexes ligated by 1,3-bis(diphenylphosphino)calix[4]arene: Preparation, X-ray structures, and catalyses. *Organometallics* **2016**, *35*, 420–427. [CrossRef]
30. Karpus, A.; Yesypenko, O.; Boiko, V.; Poli, R.; Daran, J.-C.; Voitenko, Z.; Kalchenko, V.; Manoury, E. Chiral phosphinoferrocenyl-calixarenes. *Eur. J. Org. Chem.* **2016**, *20*, 3386–3394. [CrossRef]
31. Kuhn, P.; Sémeril, D.; Jeunesse, C.; Matt, D.; Lutz, P.J.; Louis, R.; Neuburger, M. Catalytic applications of keto-stabilised phosphorus ylides based on a macrocyclic scaffold: Calixarenes with one or two pendant Ni(*P,O*)-subunits as ethylene oligomerisation and polymerisation catalysts. *Dalton Trans.* **2006**, *30*, 3647–3659. [CrossRef] [PubMed]
32. Frediani, M.; Sémeril, D.; Comucci, A.; Bettucci, L.; Frediani, P.; Rosi, L.; Matt, D.; Toupet, L.; Kaminsky, W. Ultrahigh-molecular-weight polyethylene by using a titanium calix[4]arene complex with high thermal stability under polymerization conditions. *Macromol. Chem. Phys.* **2007**, *208*, 938–945. [CrossRef]
33. Walton, M.J.; Lancaster, S.J.; Redshaw, C. Highly selective and immortal magnesium calixarene complexes for the ring-opening polymerization of *rac*-Lactide. *ChemCatChem* **2014**, *6*, 1892–1898. [CrossRef]
34. Sarkar, A.; Krishnamurthy, S.S.; Nethaji, M. Calix[4]arene bisphosphite ligands bearing two distal 2,20-biphenyldioxy or 2,20-binaphthyldioxy moieties: Conformational flexibility and allyl–palladium complexes. *Tetrahedron* **2009**, *65*, 374–382. [CrossRef]
35. Sémeril, D.; Matt, D.; Toupet, L.; Oberhauser, W.; Bianchini, C. High-pressure investigations under CO/H_2 of rhodium complexes containing hemispherical diphosphites. *Chem. Eur. J.* **2010**, *16*, 13843–13849. [CrossRef]
36. Dieleman, C.; Steyer, S.; Jeunesse, C.; Matt, D. Diphosphines based on an inherently chiral calix[4]arene scaffold: Synthesis and use in enantioselective catalysis. *J. Chem. Soc. Dalton Trans.* **2001**, *17*, 2508–2517. [CrossRef]
37. Karpus, A.; Yesypenko, O.; Boiko, V.; Daran, J.-C.; Voitenko, Z.; Kalchenko, V.; Manoury, E. Synthesis of an enantiomerically pure inherently chiral calix[4]arene phosphonic acid and its evaluation as an organocatalyst. *J. Org. Chem.* **2018**, *83*, 1146–1153. [CrossRef]
38. Arnott, G.E. Inherently chiral calixarenes: Synthesis and applications. *Chem. Eur. J.* **2018**, *24*, 1744–1754. [CrossRef]
39. Lejeune, M.; Sémeril, D.; Jeunesse, C.; Matt, D.; Lutz, P.; Toupet, L. Fast propene dimerization using upper rim-diphosphinated calix[4]arenes as chelators. *Adv. Synth. Catal.* **2006**, *348*, 881–886. [CrossRef]
40. Monnereau, L.; Sémeril, D.; Matt, D.; Toupet, L.; Mota, A.J. Efficient, nickel-catalysed Kumada-Tamao-Corriu cross-coupling with a calix[4]arene-diphosphine ligand. *Adv. Synth. Catal.* **2009**, *351*, 1383–1389. [CrossRef]
41. Monnereau, L.; Sémeril, D.; Matt, D.; Toupet, L. Cavity-shaped ligands: Calix[4]arene-based monophosphanes for fast Suzuki-Miyaura cross-coupling. *Chem. Eur. J.* **2010**, *16*, 9237–9247. [CrossRef] [PubMed]
42. Sémeril, D.; Jeunesse, C.; Matt, D. Influence des propriétes intrinsèques de ligands calixaréniques sur des réactions de transformation catalytique de l'éthylène. *Comptes Rendus Chim.* **2008**, *11*, 583–594. [CrossRef]
43. Lejeune, M.; Sémeril, D.; Jeunesse, C.; Matt, D.; Peruch, F.; Lutz, P.J.; Ricard, L. Diphosphines with expandable bite angles: Highly active ethylene dimerisation catalysts based on upper rim, distally diphosphinated calix[4]arenes. *Chem. Eur. J.* **2004**, *10*, 5354–5360. [CrossRef] [PubMed]

44. Kuhn, P.; Jeunesse, C.; Sémeril, D.; Matt, D.; Lutz, P.; Welter, R. Coordination chemistry of large diphosphanes—directional properties of a calix[4]arene proximally substituted by two−OCH_2PPh_2 podand arms. *Eur. J. Inorg. Chem.* **2004**, *2004*, 4602–4607. [CrossRef]
45. Natarajan, N.; Pierrevelcin, M.-C.; Sémeril, D.; Bauder, C.; Matt, D.; Ramesh, R. Chiral calixarene and resorcinarene derivatives. Conical cavities substituted at their upper rim by two phosphito units and their use as ligands in Rh-catalysed hydroformylation. *Catal. Commun.* **2019**, *118*, 70–75. [CrossRef]
46. Sémeril, D.; Jeunesse, C.; Matt, D.; Toupet, L. Regioselectivity with hemispherical chelators: Increasing the catalytic efficiency of complexes of diphosphanes with large bite angles. *Angew. Chem. Int. Ed.* **2006**, *45*, 5810–5814. [CrossRef]
47. Gagnon, J.; Vézina, M.; Drouin, M.; Harvey, P.D. Regioselective upper-rim functionalizations of calix[4]arene by diphenylphosphino groups. *Can. J. Chem.* **2001**, *79*, 1439–1446. [CrossRef]
48. Jaime, C.; de Mendoza, J.; Prados, P.; Nieto, P.M.; Sanchez, C. Carbon-13 NMR chemical shifts. A single rule to determine the conformation of calix[4]arenes. *J. Org. Chem.* **1991**, *56*, 3372–3376. [CrossRef]
49. Liu, S.; Sandoval, C.A. Evaluation of calix[4]arene-based chiral diphosphite ligands in Rh-catalyzed asymmetric hydrogenation of simple dehydroamino acid derivatives. *J. Mol. Catal. A Chem.* **2010**, *325*, 65–72. [CrossRef]
50. Diéguez, M.; Ruiz, A.; Claver, C. Chiral diphosphites derived from D-glucose: New highly modular ligands for the asymmetric catalytic hydrogenation. *J. Org. Chem.* **2002**, *67*, 3796–3801. [CrossRef]
51. Kostas, I.D.; Vallianatou, K.A.; Holz, J.; Börner, A. Rhodium complexes with a new chiral nitrogen containing BINOL-based diphosphite or phosphonite ligand: Synthesis and application to hydroformylation of styrene and/or hydrogenation of prochiral olefins. *Appl. Organomet. Chem.* **2005**, *19*, 1090–1095. [CrossRef]
52. Li, Y.; Ma, B.; He, Y.; Zhang, F.; Fan, Q.-H. Chiral metallacrown ethers for asymmetric hydrogenation: Alkali-metal ion mediated enhancement of enantioselectivity. *Chem. Asian J.* **2010**, *5*, 2454–2458. [CrossRef]
53. Cai, C.; Deng, F.; Sun, W.; Xia, C. New bidentate phosphorus ligands based on a norbornane backbone for rhodium-catalyzed asymmetric hydrogenation. *Synlett* **2007**, *19*, 3007–3010. [CrossRef]
54. Chan, A.S.C.; Pluth, J.J.; Halpern, J. Identification of the enantioselective step in the asymmetric catalytic hydrogenation of a prochiral olefin. *J. Am. Chem. Soc.* **1980**, *102*, 5952–5954. [CrossRef]
55. Halpern, J. Mechanism and stereoselectivity of asymmetric hydrogenation. *Science* **1982**, *217*, 401–407. [CrossRef]
56. Landis, C.R.; Halpern, J. Asymmetric hydrogenation of methyl-(*Z*)-α-acetamidocinnamate catalyzed by {l,2-bis((phenyl-*o*-anisoyl)phosphino)ethane}rhodium(I): Kinetics, mechanism, and origin of enantioselection. *J. Am. Chem. Soc.* **1987**, *109*, 1754–1757.
57. Sarkar, A.; Nethaji, M.; Krishnamurthy, S.K. Phosphite ligands derived from distally and proximally substituted dipropyloxy calix[4]arenes and their palladium complexes: Solution dynamics, solid-state structures and catalysis. *J. Organomet. Chem.* **2008**, *693*, 2097–2110. [CrossRef]
58. Liu, W.; Das, P.J.; Colquhoun, H.M.; Stoddart, J.F. Whither Second-Sphere Coordination? *CCS Chem.* **2022**, *4*, 755–784. [CrossRef]